VOL. 17, NO. 17, SEPTEMBER 2022 ISSN 1819-6608
ARPN Journal of Engineering and Applied Sciences

www.arpnjournals.com

HYDRODYNAMICS AND STRUCTURAL MECHANICS OF JET PUMPS IN A BOILING WATER REACTOR: LEAKTRANSIENT ANALYSIS IN A JET PUMP

G. Espinosa-Paredes[1], A. Nuñez-Carrera[2], J. R. Varela-Ham[1], E.-G. Espinosa-Martínez[3], A. Vázquez-Rodríguez[1], J. Centeno-Perez[1], M. A. Polo-Labarrios[3], H. Sánchez-Mora[4] and S. Quezada-Garcia[3]
[1]Energy Resources Engineering Area, Metropolitan Autonomous University-Iztapalapa, Mexico City, Mexico
[2]Commission for Nuclear Safety and Safeguards, Mexico City, Mexico
[3]Faculty of Engineering, National Autonomous University of Mexico, Mexico City, Mexico
[4]Higher School of Physics and Mathematics, National Polytechnic Institute, Mexico City, Mexico
E-Mail: sequga@gmail.com

ABSTRACT

The failure of a jet pump may produces a leakage in the slip joint or a rupture in the riser pipe. The failure occurs when the jet pumps are out of the range of their natural frequency. The aim of this work is study the reactor safety operation under the failure of a jet pump through the transient analysis. This work presents four scenarios that correspond to the severity of the jet-pump failure. The behavior of essential variables such as: power reactor, reactor water level, water mass flow rate in the core and recirculation, among others, are analyzed. The results show that the reactor self-controls without the need of the operator intervention in less than 20 seconds. When the failure is 100%, the power reactor decreases about 20% in approximately one and a half seconds and stabilizes at 94% of the nominal power. The mass flow in the core is stabilized above 96%. The total core flow is the most significant parameter in case the jet pumps failure for long period.

Keywords: boiling water reactor, jet pump, slip joint, riser pipe, transient analysis.

Nomenclature

a	Inertial coefficient, m^{-1}
A	Flow area, m^2
b	Inertial coefficient, m^{-1}
c_i	Delayed neutron concentration of the i-th precursor (normalized), dimensionless
C_{f0}	Single-phase friction factor, dimensionless
Cp	Specific heat capacity, J kg^{-1} K^{-1}
CR	Control rod position, dimensionless
d	Inertial coefficient, m^{-1}
D_h	Hydraulic diameter, m
g	Acceleration of gravity, m s^{-2}
G	Mass flux, kg m^{-2} s^{-1}
h	Enthalpy, J kg^{-1}
j	Drift flux, m s^{-1}
K	Hydraulic loss coefficient, m^{-4}
k	Thermal conductivity, W m^{-1} K^{-1}
n	Neutron density (normalized), dimensionless
N	Core nodes, dimensionless
m	Mass, kg
p	Pressuere, Pa
P	Reactor power, W
P_H	Heated perimeter,m
P_0	Nominal power, W
q''	Heat flux, W m^{-2}
r	Radial coordinate, m
t	time, s
T	Temperature, K
$\bar{T}_m$	Average moderator temperature, K
$\bar{T}_U$	Average fuel temperature, K
V_U	Fuel volume in a fuel rod, m^3
W	Mass flow, kg s^{-1}
x	Vapor quality, dimensionless
z	Axial coordinate, m

Greek symbols

β	Total fraction of delayed neutron, dimensionless
ε	Void fraction, dimensionless
$\bar{\varepsilon}$	Average void fraction, dimensionless
Δp	Drop pressure, Pa
Δz	Core node length, m
Γ	Volumetric vapor generation rate, kg $m^{-3}s^{-1}$
Λ	Prompt neutron generation time, s
λ	Decay constant, s^{-1}
ρ	Density, kg m^{-3}
ρ_{cr}	Density due to reactor control rods, pcm
ρ_D	Reactivity due toDoppler effect, pcm
ρ_{Rx}	Reactivity, pcm
ρ_{xe}	Reactivity due to xenon concentration, pcm
ρ_ε	Reactivity due to the void fraction, pcm
ϕ_{f0}	Two-phase multiplier, dimensionless
$\Psi(z)$	Axial power factor, dimensionless

List of subscripts

b	Recirculation pump
br	Failure to break in a jet pump
c	Core
CL	Clad
d	Driver
dif	Diffusor
f	Saturated liquid
g	Saturated vapor
gr	Gravity
jp	Jet pump
jpt	Jet pump throat
l	Liquid phase

lr1	Jet pump loop A
lr2	Jet pump loop B
m	Mixture
RRS	Recirculation
r	Recirculation
sep	Steam separators
sjpi	Suction jet pump
U	Nuclear fuel
v	Vapor phase
1	Loop recirculation A
2	Loop recirculation B

INTRODUCTION

The jet pumps failure analysis use the coupling of the hydrodynamics and the structural analysis in a typical BWR was performed by Espinosa-Paredes *et al*. (2020). The liquid in the jet pump is accelerated due to high differential pressure in the nozzle that induces vibrations in the slip joint of the diffuser. If the vibrations are out of the range of the natural frequency may produce a leakage in the slip joint or a rupture in the riser pipe. The hold-down beam assemblies and subsequent jet pump function may degrade significantly during operation. This potential degradation could lead to jet pump disassembly and possibly reduce the safety margin during postulated accidents (USNRC, 1980).

Comprehensive safety analysis is required for prediction of anuclear reactor behavior in either steady-state or transient modes, thus, numerical codes are developed and applied (e.g., Espinosa-Paredes *et al*., 2006; Zhang & Xie, 2017; Lu & Xie, 2019; Mazaher *et al*., 2019; Takeda *et al*. 2020). Toguarantee nuclear reactors safety, numerical codes allowperform transient analysis underabnormal operation conditions, such as the one discussed in this work, abnormaljet pump condition.

This work analyzes a BWRtransient behavior in a jet pump failure event with different degrees of severity. The failure of a jet pump due to hydrodynamic vibrations, when they are out of the range of their natural frequency, may produces a leakage in the slip joint or a rupture in the riser pipe as was demonstrated in a previous work of Espinosa-Paredes *et al.* (2020). This analysis is performed by conducting numerical simulations using a numerical code developed by Espinosa-Paredes *et al.* (2006). The jet pump failure is modeled in the BWR reactor recirculation system, as well as the effects on the reactor vessel model, which is implemented in the numerical code. The essential variables of nuclear reactor such as thermal power, reactor pressure, reactor water level, void fraction, water flow in the core, drive flow, pressure drop in the core and feed water flow are analyzed and discussed.

LEAKAGE FLOW MODEL IN JET PUMPS

The BWR configuration and the flow paths are illustrated in Figure-1. The reactor recirculation system (RRS), whose objective is to circulate the required coolant flow through the reactor core and consists of two external loops to the reactor vessel. Each loop contains a pump with a directly coupled motor, a control valve flow, and two shut-off valves. The jet pump located within the reactor vessel provides a continuous internal circulation path for a major portion of the core coolant flow. The recirculation pumps take the suction from the downward flow in the annulus between the core shroud and the vessel wall. The core flow is taken from the vessel through two recirculation nozzles. Into this site, the flow is pumped to a higher pressure, distributed through a manifold where several riser pipes are connected, and returned to the vessel inlet nozzles. This flow is discharged from the jet pump nozzles into the initial stage of the jet pumps throat, where, due to a momentum exchange process, induces the surrounding water in the downcomer region to be drawn into the jet pumps throats. Here, these two flows are mixed and then diffused in the diffuser, to be finally discharged into the lower core plenum. The coolant water passes along the individual fuel rods inside the fuel channel where it boils and becomes a two-phase steam/water mixture. In the core, the two-phase fluid generates upward flows through the axial steam separators while the steam continues through the dryers and flows directly out through the steam lines into the turbine-generator.

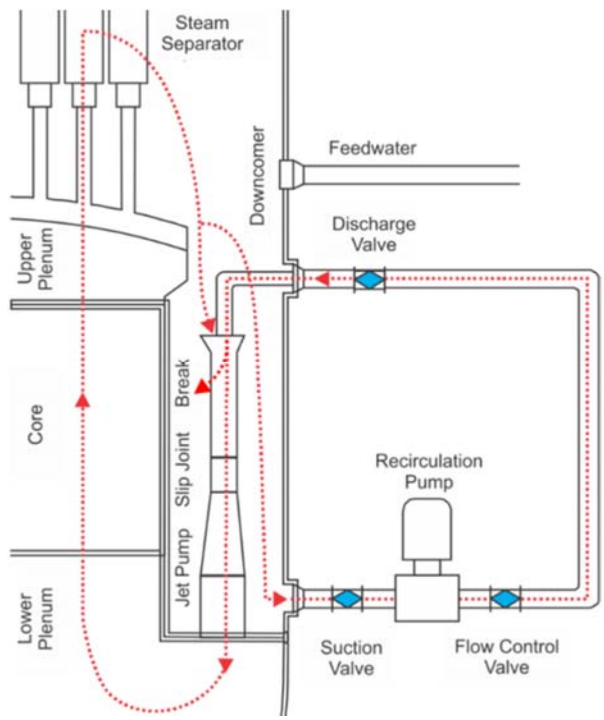

Figure-1. Rising pipe break (jet pump) in the BWR reactor recirculation system.

The condensate flow is then returned through the feedwater heaters by the condensate-feedwater pumps into the vessel. The water, which is separated from the steam in the steam separators, flows downward in the periphery of the reactor vessel and mixes with the incoming main feed flow from the turbine. This downward flow enters to the jet pumps and the remainder exits from the vessel as recirculation flow. Furthermore, the flow pathway by raiser breaks as shown in Figure-1. The break in the jet

VOL. 17, NO. 17, SEPTEMBER 2022 ISSN 1819-6608
ARPN Journal of Engineering and Applied Sciences

pump riser can be caused by flow instability in the slip joint.

To obtain the momentum balances, the system model includes the pressure drops and flows from the downcomer, recirculation pumps, nozzles, jet pumps throat and diffuser, lower and upper plenum, reactor core and steam separators. Then, the mass flow rate entering the core is given by:

$$W_c = W_{lr1} + W_{lr2} \tag{1}$$

where the first right-hand side term corresponds to the mass flow rate discharged from the jet pump loop “A”, while the second right hand-side term is the mass flow rate of the jet pump loop “B”. The momentum balances to the internal and external circuits, the flows through the jet pumps are given by:

$$\frac{dW_{lr1}}{dt} = \frac{b\Delta p_{RRS2} - a\Delta p_{RRS1}}{b^2 - a^2} \quad \text{for loop A} \tag{2}$$

$$\frac{dW_{lr2}}{dt} = \frac{b\Delta p_{RRS1} - a\Delta p_{RRS2}}{b^2 - a^2} \quad \text{for loop B} \tag{3}$$

where t is the time, a and b are the inertial coefficients and Δp_{RRS} is the rector recirculation system pressure drop with leakage flow due to the riser pipe break, that is given by:

$$\begin{aligned}\Delta p_{RRSi} &= \left(\Delta p_{jp} + \frac{W_{lri}^2}{2A_{jpt}^2\rho_r} - \frac{W_{sjpi}^2}{2A_{sjpi}^2\rho_r}\right)\frac{W_{sjp}}{W_d} - K_{sjpi}\frac{W_{sjpi}^2}{\rho_r} \\ &+ K_{dif}\frac{W_{lri}^2}{\rho_r} - \underbrace{K_{br}\frac{W_{br}^2}{\rho_r}}_{\text{Jet pump leak}} - \Delta p_{sep} + \Delta p_{gr} - \Delta p_c, \quad i = 1,2\end{aligned} \tag{4}$$

where A is the flow area, K is the hydraulic loss coefficient, p is the pressure andρ is the density. The subscripts *jp*, *jpt* and *sjpi* refer to jet pump, jet pump throat and suction jet pump, respectively. While the subscripts r, d, *dif*, *br*, *sep*, *gr* and$c$ refer to recirculation, driver, diffusor, failure to break in a jet pump, steam separators, gravity and core, respectively.

The rising pipe break that produces a leakage flow W_{br} in the jet pump, was estimated to be turbulent flow, i.e., it does not reach critical flow conditions. The leakage flow discharges into the annular region of the reactor core, affecting, among other essential variables, the reactor water level. The hydraulic coefficient due to jet pump failure, K_{br}, is a function of the severity, i.e., 0% means there is no failure and 100% means that the rising pipe has been broken in shear. The jet pressure raise is given by:

$$\text{D}p_{jpi} = \frac{W_{di}^2}{A_{jpt}A_d r_r} + \frac{W_{sjpi}^2}{A_{jpt}A_{sjp} r_r} - \frac{W_{lri}^2}{A_{jpt}^2 r_r} \tag{5}$$

The total core pressure drop is the sum of the frictional, acceleration and gravitational components:

$$\Delta p_c = -\sum_{j=1}^{N}\left[\frac{\phi_{f0,j}^2 2C_{f0}W_c^2\Delta z}{A_c^2 D_h \rho_f} + \frac{W_c^2}{A_c^2}\left(\frac{1}{\rho_{c,j+1}} - \frac{1}{\rho_{c,j}}\right) + \rho_{c,j} g\Delta z_j\right] \tag{6}$$

where N is the total number of nodes in the core, C_{f0} is single-phase friction factor, Δz is core node length, D_h is hydraulic diameter, g is acceleration of gravity and $\phi_{f0}$is two-phase multiplier, that is given by (Wallis, 1969):

$$\phi_{f0}^2 = 1 + x\left(\frac{\rho_f}{\rho_g} - 1\right) \tag{7}$$

where x is the vapor quality, the subscripts f and g refer to saturated liquid and saturated vapor, respectively.

The drive flow is given by:

$$\frac{dW_{di}}{dt} = \frac{1}{d}\left[\left(K_{sjp} + \frac{1}{2A_{sjp}^2}\right)\frac{W_{sjpi}^2}{\rho_r} + \Delta p_{bi} - \left(K_r + \frac{1}{2A_d^2}\right)\frac{W_{di}^2}{\rho_r}\right] \tag{8}$$

where d is an inertial term, Δp_{bi} is the pressure drop in the recirculation pump, K_{sjp} is the hydraulic loss coefficient due the frictional force in the suction jet pump and K_r is due the frictional force in the recirculation system, which is function of the flow control valve position.

IMPLEMENTATION

To analyze the transient effect due to break in a jet pump, the leakage flow model, developed in the previous section, was implemented in the BWR numerical code developed by Espinosa-Paredes *et al*. (2006). This model was based on lumped and distributed parameters approximations, which includes the vessel dome and the downcomer, the recirculation loops, the neutron process, the fuel pin temperature distribution, the core lower and upper plenums and the pressure and level controls. The thermal-hydraulic model that describes the dynamic behavior of the lower and upper plenums and the reactor core, as well as the fuel temperature model, were based on distributed parameters approximation. The vessel dome, downcomer, recirculation loops and neutron process models were based on the lumped parameters approximation as well.

The thermal-hydraulic model consists of five equations model, which are based on liquid and gas phases, mass balances, mixture momentum, mixture energy and liquid phase energy:

ARPN Journal of Engineering and Applied Sciences

$$\frac{\partial}{\partial t}(\rho_g \varepsilon_g) + \frac{\partial}{\partial z}(j_g \rho_g) = \Gamma \tag{9}$$

$$\frac{\partial}{\partial t}(\rho_l \varepsilon_l) + \frac{\partial}{\partial z}(j_l \rho_l) = -\Gamma \tag{10}$$

where ε is void fraction, j is the drift flux and Γ is volumetric vapor generation rate.

$$\frac{\partial}{\partial t}(\rho_g h_g \varepsilon_g) - \varepsilon_g \frac{\partial p}{\partial t} + \frac{\partial}{\partial z}(\rho_g h_g j_g) = \frac{q'' P_H}{A_c} - \Gamma h_g \tag{11}$$

$$\frac{\partial}{\partial t}(\rho_l h_l \varepsilon_l) - \varepsilon_l \frac{\partial p}{\partial t} + \frac{\partial}{\partial z}(\rho_l h_l j_l) = \frac{q'' P_H}{A_c} - \Gamma h_f \tag{12}$$

where h is enthalpy, $q''$is the heat flux and P_H is the heated perimeter.

$$\frac{\partial}{\partial t}(\rho_m h_m) - \frac{\partial p}{\partial t} + G_m \frac{\partial h_m}{\partial z} = \frac{q'' P_H}{A_c} \tag{13}$$

where G is mass flux. The properties of the mixture are calculated from:

$$\rho_m = \rho_g \varepsilon_g + \rho_l \varepsilon_l \tag{14}$$

$$G_m = \rho_g j_g + \rho_l j_l \tag{15}$$

$$\rho_m h_m = \rho_g h_g \varepsilon_g + \rho_l h_l \varepsilon_l \tag{16}$$

The drift flux approach (Zuber and Findlay, 1965) is applied to consider relative velocity, and subcooled boiling was considered using Saha and Zuber's (1974) approximation. Depending on the mixture enthalpy, h_m, the following two cases were considered: When $h_f<h_m<h_g$ is two-phase saturated; when $h_m<h_f$ and$h_l<h_f$. Liquid-phase occurs first and, subsequently, subcooled boiling appears.

The vessel dome is modelled as a two-region volume, one region being liquid and the other vapor. The two regions are assumed to be at the same pressure but not necessarily at the same temperature (Robinson *et al*., 1983):

$$\frac{dp_{Rx}}{dt} = -\frac{\dfrac{1}{\rho_l}\dfrac{dm_l}{dt} + \dfrac{1}{\rho_v}\dfrac{dm_v}{dt} + \left(\dfrac{\partial \rho_l^{-1}}{\partial h_l}\right)_p \displaystyle\sum_i W_{li}(h_{il} - h_l)}{m_l\left[\dfrac{1}{\rho_l}\left(\dfrac{\partial \rho_l^{-1}}{\partial h_l}\right)_p + \left(\dfrac{\partial \rho_l^{-1}}{\partial p}\right)_{h_l}\right] + m_v\left(\dfrac{\partial \rho_v^{-1}}{\partial p}\right)_{h_v}} \tag{17}$$

where m is the mass, the subscripts l and v refer to liquid phase and vapor phase, respectively. The enthalpy of liquid h_l and enthalpy of vapour h_v are given by the following balance equations:

$$\frac{dm_l}{dt} = \sum_i W_{li} + W_{br} \tag{18}$$

$$\frac{dm_v}{dt} = \sum_i W_{vi} \tag{19}$$

$$\frac{dh_l}{dt} = \frac{1}{m_l}\sum_i W_{li}(h_{li} - h_l) + \frac{1}{\rho_l}\frac{dp}{dt} + \frac{W_{br}}{m_l}(h_{br} - h_l) \tag{20}$$

The recirculation model includes the pressure drops and flows from the downcomer, recirculation pumps, nozzles, jet pumps throat and diffuser, lower and upper plenum, reactor core and steam separators, in order to obtain the momentum balances (The recirculation system flow path is shown in Figure-1, which includes the rising pipe break). The Feedwater System (FW) and Main Steam Line (MSL) models are considered as dummy or auxiliary models. The formulation of these models are based on resistive node approach. The reactor model is completed by including control models. In addition, this model uses a set of empirical correlations valid for the normal range of BWR operating conditions.

The reactor power is given by

$$P(t,z) = n(t)\Psi(z)P_0 \tag{21}$$

where $\Psi(z)$ is the axial power factor, P_0 is nominal power and $n(t)$ is the neutron density (normalized), which is calculated from a point reactor kinetics model with six groups of delayed neutrons:

$$\frac{dn(t)}{dt} = \frac{\rho_{Rx}(t) - \beta}{\Lambda} n(t) + \sum_{i=1}^{6} \lambda_i c_i(t) \tag{22}$$

Where ρ_{Rx} is the reactivity, β is the total fraction of delayed neutron, Λ is the prompt neutron generation time, λ is the decay constant and c is the delayed neutron concentration of the precursor, which can be calculated from:

$$\frac{dc_i(t)}{dt} = \frac{\beta_i}{\Lambda} n(t) + \lambda_i c_i(t)\,;\; i = 1,2,...,6 \tag{23}$$

The net reactivity of the nuclear reactor includes four main components: feedback reactivity due to the void fraction in two-phase flow ρ_ε, Doppler effect ρ_D due to fuel temperature, poison due to xenon concentration ρ_{xe}, and reactor control rods ρ_{cr}. Then, the reactor feedback reactivities are the sum of each of these contributions:

$$\rho_{Rx}(t) = \rho_\varepsilon(\bar{\varepsilon}_g) + \rho_D(\bar{T}_U) + \rho_m(\bar{T}_m) + \rho_{cr}(CR) \tag{24}$$

where $\bar{T}_U$ is the average fuel temperature, $\bar{\varepsilon}_g$ is the average void fraction, $\bar{T}_m$ is the average moderator temperature, and CR is the control rod position.

ARPN Journal of Engineering and Applied Sciences

A detailed multi-node fuel pin model is based on transient temperature distribution in the fuel pin:

$$\left(\rho Cp\right)_U \frac{\partial T_U}{\partial t} = k_U \frac{1}{r}\frac{\partial}{\partial r}\left(r\frac{\partial T_U}{\partial r}\right) + \frac{P(t,z)}{V_U} \tag{25}$$

and clad of the fuel

$$\left(\rho Cp\right)_{CL} \frac{\partial T_{CL}}{\partial t} = k_{CL} \frac{1}{r}\frac{\partial}{\partial r}\left(r\frac{\partial T_{CL}}{\partial r}\right) \tag{26}$$

where Cp is the specific heat capacity, T is the temperature, k is the thermal conductivity, V_U is the fuel volume in a fuel rod. The subscripts U and CL refer to nuclear fuel and clad, respectively.

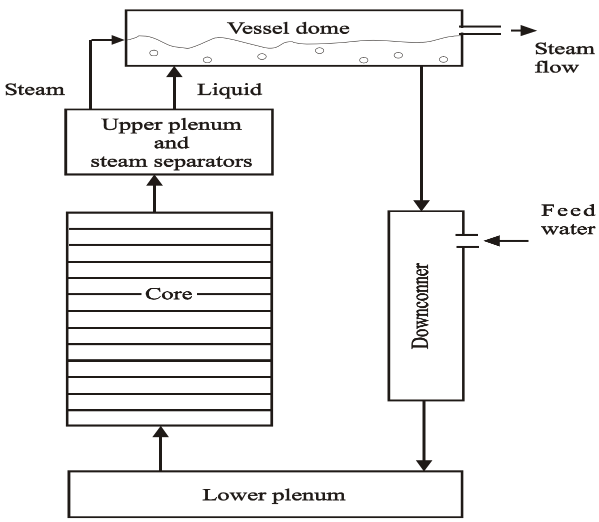

Figure-2. Nodalization of a simplified BWR model.

Figure-2 is a schematic diagram of the boiling water reactor where the arrangement of the computational cells of the BWR model is shown. The reactor vessel was divided into five zones. Two of these zones, the vessel dome and the down comer, have a variable volume according to the vessel water level. The three fixed volume zones are the lower plenum (which includes the jet pump volume), the upper plenum and steam separators, and the reactor core. Due to its importance on model performance, the latter component was subdivided into twelve one-dimensional nodes.

TRANSIENT ANALYSIS

This work assumes that the vibrations in the jet pump provoke a rupture in the riser of one jet pump in the loop A. The transient analysis considers four scenarios: ruptures of 25%, 50%, 75% and 100% (guillotine rupture), which is compared with normal operation. The numerical simulations were carried out at 100% of the reactor's nominal power.

Figures 3-10 presents the simulated behavior of the essential variables in a BWR. In these figures, the dotted line corresponds to normal operation, i.e., no leak in the jet pump; and red, blue, green and pink lines were used to indicate the behavior of the essential variable at 25%, 50%, 75% and 100% of break in the jet pump, which correspond to break area A_B.

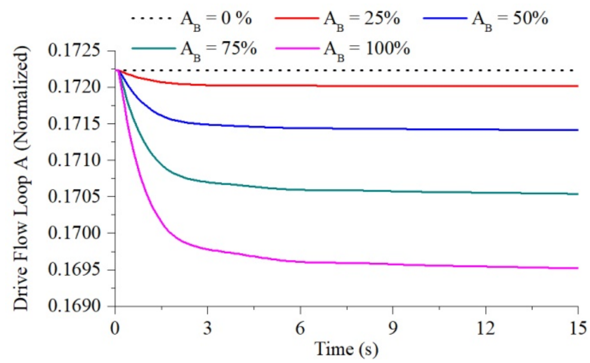

Figure-3. Drive flow in the loop A: W_{d1}.

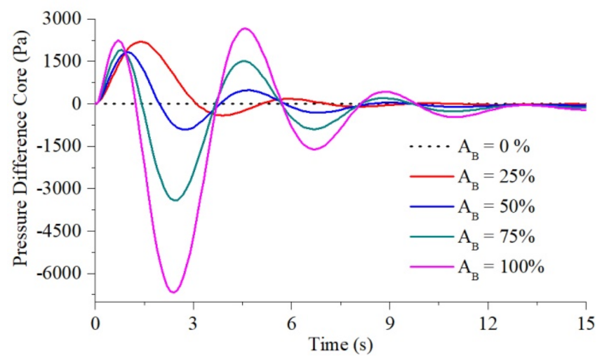

Figure-4. Pressure difference in the core: $\Delta P_c - \Delta P_{c0}$.

The sudden leakage (Figure-3) in the jet pump introduces a perturbation in the differential pressure in the reactor core as depicted in Figure-4. The higher oscillation is observed when the leakage is 100%. The oscillation is damped after 15 s of the transient. In Figure-6 it can be observed that the reduction in the drive flow in the loop A caused by the rupture of the jet pump depicted in Figure-3. The higher reduction is observed at A_B=100% and corresponds to 1.6% of the nominal core flow. The loss of the resistance in the loop A increases the flow in the loop B (about 0.5%) for the case of total rupture in the jet pump (A_B=100%) as depicted in Figure-5. Due to this phenomenon it is easy to identify the loop associated with the failure of the jet pump.

Figure-6 shows the reduction of the core flow is a consequence of the reduction in the driving flow when the leakage in the jet pump started. The higher reduction is about 4% when the rupture in the jet pump is maximum, A_B=100%.

ARPN Journal of Engineering and Applied Sciences

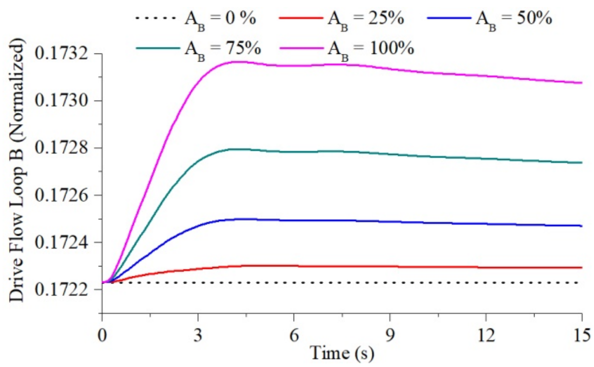

Figure-5. Drive flow in the loop B: W_{d2}.

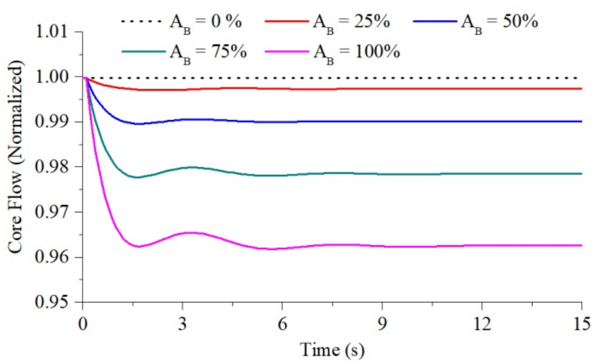

Figure-6. Core flow: W_c.

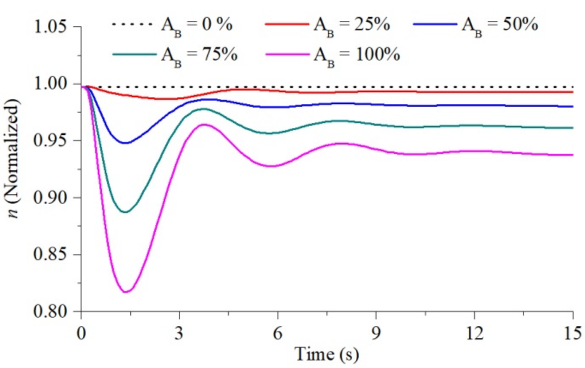

Figure-7. Neutron density (Reactor power): $n(t)$.

The transient behavior of the neutron density, which is directly proportional to the power of the reactor, for different degrees of severity in a jet pump breakage is depicted in Figure-7.

From a reactor operation point of view, the reactor operator will observe a drastic decrease in power, and for 100% damage to the jet pump it will decrease approximately 6%, without affecting the operation of the reactor, and without risk to safety. Besides the reactor operator can observe the reduction of the core flow (Figure-6).

The loss of driving flow due to leaking in the jet pump increases the void fraction in the reactor core, therefore the number of fissions decrease (Figure-7). In case of a total failure of the jet pump (A_B=100%) the neutron flow decreases until 83% when the reactor is operated at rated power. The behavior of the neutron flow is consistent with the report of Dresden U3, Pilgrim U1 and Quad Cities U2 (USNRC, 1980; USNRC, 1993).

The increase of void fraction in the reactor core (Figure-8) due to the reduction of the core flow results in an increase in the reactor water level (Figure-9). The higher increase is obtained when the jet pump has total break (A_B=100%). In this case the increase in the water level is about 0.2% over the normal level. The reduction of the core flow (Figure-6) increases the void fraction in the core of the reactor. An increase of 1.6% is the higher and corresponds to the case of total rupture in the jet pump (A_B=100%). The feed water control system of the reactor follows the water level in the vessel (Figure-10). The increase in the reactor level has an inverse behavior of the feedwater, the reduction of feedwater is about 22% when the vessel reaches the maximum level at about 1.7 s.

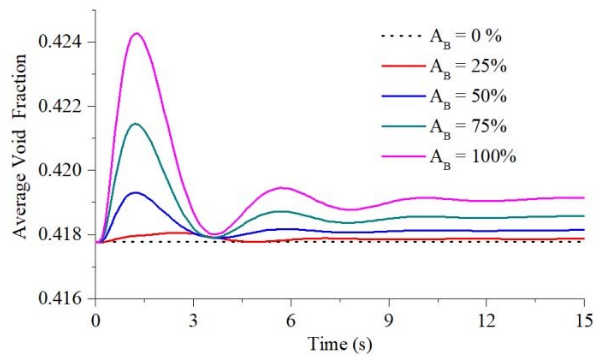

Figure-8. Average void fraction in the reactor core: $\overline{\varepsilon}_g$

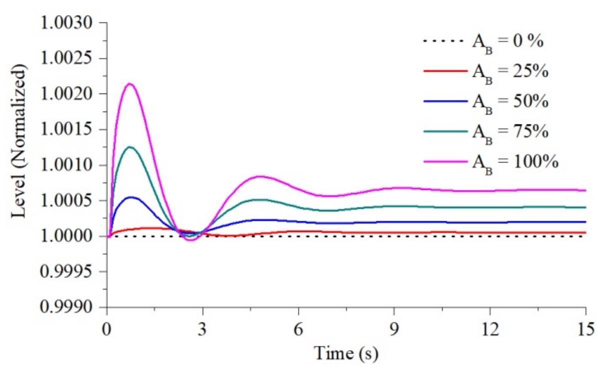

Figure-9. Water level in the reactor vessel: N_L.

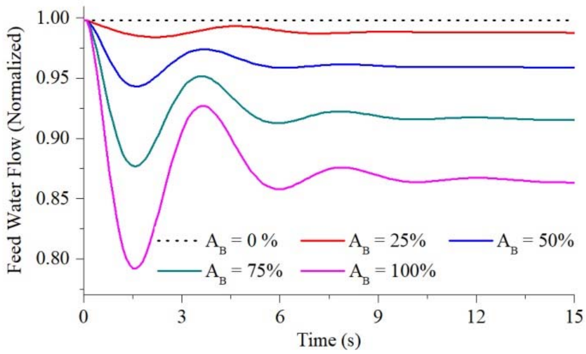

Figure-10. Feed water flow.

CONCLUSIONS

The transient analysis due to failure of a jet pump was carried out in this work. Four failures were postulated and analyzed: 25%, 50%, 75% and 100%. In all cases the reactor self-controls without the need of the operator intervention in less than 20 seconds (Figures 3-10). The operator of a BWR nuclear power plant will not observe significant changes in the behavior of the reactor (almost imperceptible) with a failure of the order of 25% in the jet pump. When the failure is about 100%, it can be observed a power overshoot decrease of the order of 20% in about one and a half seconds (Figure-7), but finally stabilizing at 94% of rated power. The mass flow rate in the core is stabilized above 96% (Figure-6). According with the transient simulations, the total core flow is the most significant parameter to be observed by the reactor operator in case of the jet pump failure for long period of time.

The simulated results show that the failure of a jet pump does not affect the integrity in the safe operation of a BWR reactor and is not needed the operation with only one recirculation loops (Single Loop Operation-SLO, General Electric, 2004). The reduction of the core flow is only 4% below of the rated power and it is far away to induce potential density waves oscillation.

REFERENCES

Espinosa-Paredes G., Núñez-Carrera A. and Vázquez-Rodríguez A. 2006. Simplified distributed parameters BWR dynamic model for transient and stability analysis. Annals of Nuclear Energy. 33, 1245-1259.

Espinosa-Paredes G., Centeno-Pérez J., Núñez-Carrera A., Quezada-García S., Vázquez-Rodríguez A., Espinosa-Martínez, E. G. 2020. Hydrodynamics and structural mechanics of jet pumps in a boiling water reactor. ARPN Journal of Engineering and Applied Sciences (Submitted).

General Electric GE-NE-0000-0027-5301a Revision 1. DRF 0000-0027-4472 Clase I, July 2004. Pilgrim Nuclear Power Plant Station Single Loop Operation. Non-proprietary version.

Lu M. and Xie H. 2019. A numerical investigation of SBLOCA scenario in nuclear heating reactor. Journal of Nuclear Science and Technology. 56(8): 731-743.

Mazaher M. G., Salehi A. A. and Vosoughi N. 2019. Implementation of a dynamic Monte Carlo method for transients analysis with thermal-hydraulic feedbacks using MCNPX code. Annals of Nuclear Energy. 130, 240-249.

Robinson J. T., Sehgal R. and Todreas N. 1983. Analysis of loss of feed water ATWS transient. Proc. 2ndInt. Topl. Mtg. Nuclear Reactor Thermal-Hydraulics, Santa Barbara, California, p. 537, American Nuclear Society.

Saha P. and Zuber N. 1974. Point of net vapor generation and vapor void fraction in subcooled boiling. Proceedings of Fifth Int. Heat Transfer Conf.

Takeda S., Takeda T., Fuchita S. and Kitada T. 2020. Development of an improved quasi-static transient analysis code based on three-dimensional Sn nodal transport theory for fast reactor. Annals of Nuclear Energy. 143, 10749.

USNRC. 1980. IEB 80-07 BWR Jet Pump Assembly Failure (Generic Letter 80-27). SSINS No.: 6820 Accession No.: 8002280648. WASHINGTON, D.C. 20555.

USNRC. 1993. Information Notice No. 93-101: Jet Pump Hold-Down Beam Failure. WASHINGTON, D.C. 20555.

Wallis G. B. 1969. One-Dimensional Two-Phase Flow, McGraw-Hill Book Company, New York.

Zhang G. and Xie H. 2017. Comparison and analysis on transient characteristics of integral pressurized water reactors. Annals of Nuclear Energy. 104, 91-102.

Zuber N. and Findlay J. A. 1965. Average volumetric concentration in two-phase flow systems. J. Heat Transfer. 87, 453-468.